AC Electrokinetics of conducting microparticles: A review

Antonio Ramos, Pablo García -Sánchez, Hywel Morgan

PII: S1359-0294(16)30076-0
DOI: doi: 10.1016/j.cocis.2016.06.018
Reference: COCIS 1056

To appear in: *Current Opinion in Colloid & Interface Science*

Received date: 6 May 2016
Revised date: 27 June 2016
Accepted date: 29 June 2016

Please cite this article as: Ramos Antonio, ~~a-Sánchez Pablo Garc~~, Morgan Hywel, AC Electrokinetics of conducting microparticles: A review, *Current Opinion in Colloid & Interface Science* (2016), doi: 10.1016/j.cocis.2016.06.018

AC Electrokinetics of conducting microparticles: a review[1]

Antonio Ramos, Pablo García-Sánchez

University of Seville, Spain

Hywel Morgan

University of Southampton, UK

Abstract

This paper reviews both theory and experimental observation of the AC electrokinetic properties of conducting microparticles suspended in an aqueous electrolyte. Applied AC electric fields interact with the induced charge in the electrical double layer at the metal particle-electrolyte interface. In general, particle motion is governed by both the electric field interacting with the induced dipole on the particle and also the induced-charge electro-osmotic (ICEO) flow around the particle. The importance of the RC time for charging the double layer is highlighted. Experimental measurements of the AC electrokinetic behaviour of conducting particles (dielectrophoresis, electro-rotation and electro-orientation) are compared with theory, providing a comprehensive review of the relative importance of particle motion due to forces on the induced dipole compared with motion arising from induced-charge electro-osmotic flow. In addition, the electric-field driven assembly of conducting particles is reviewed in relation to their AC electrokinetic properties and behaviour.

Keywords: AC electrokinetics, induced charge electrophoresis, dielectrophoresis, metallic microparticles

[1]Dedicated to the memory of Prof. Antonio Castellanos (March 1947-Jan 2016), who inspired so many of us.

1. Introduction

The use of AC electric fields for manipulating and characterising small particles in suspension is well-known [1, 2] and many applications have appeared over the last decades in fields such as colloidal science and biotechnology. More recently, the manipulation of metal and semiconducting particles has been explored in the context of microfluidics and nanoelectronics. The use of AC electrokinetic methods for the rapid and precise control of particle assembly has been used for bottom-up fabrication of engineered microstructures. One example includes the formation of microwires between electrodes by assembling metallic nanoparticles from suspension [3, 4]. The chaining of metallodielectric Janus spheres has also been demonstrated [5, 6]. The research community is also exploring the use of nanowires and nanotubes as biosensors [7], as building blocks for novel nanocircuits [8], and/or elements of dense arrays for light absorption in solar cells [9]. Experimental work has proven the ability of AC electric fields to position and rotate nanowires [10–12]. Krupke *et al* [13] demonstrated the separation of semiconducting from metal carbon nanotubes. Reversible assembly of patterns of metal nanowires has also been demonstrated using AC fields [14].

In this review article, we focus on the effects of AC electric fields on conducting microparticles suspended in aqueous electrolytes. We summarise the more relevant experimental papers and clarify the underlying mechanisms that give rise to the observed motion of conducting microparticles. Importantly, we show that the charging of the electrical double layer (EDL) is the interfacial polarization mechanism responsible for particle behaviour. This is in contrast with early publications where conducting particles in electrolytes have often been incorrectly characterized by a finite conductivity and permittivity, ignoring the double-layer polarization at the metal-electrolyte interface [15–18]. This simplistic model predicts positive polarizabilities for all frequencies in the quasi-electrostatic regime and cannot explain the experimental observations of electrorotation and electroorientation spectra of metallic particles [11, 19, 20].

Furthermore, the inclusion of the EDL charging implies that the motion of the particles is not only generated by the electrical forces on the induced dipole (or multipoles), but electroosmotic slip velocities on the particle surface play an important role. The AC electrokinetic behavior of conducting particles turns to be a very interesting problem from a fundamental point of view. We will show situations where the particle velocity is measured for a known EDL potential. This implies that the induced zeta potential can be determined from the velocity measurement, while the voltage drop across the double layer is known, allowing for a direct comparison with standard electrokinetic theory. The paper begins with a qualitative analysis of the electrical response of a conducting particle in an electrolyte followed by a description of the induced motion on this particle.

1.1. Polarization of a conducting particle

When an uncharged conducting particle is suddenly exposed to an electric field, electrons in the conductor move almost instantaneously so as to make the electric field inside equal to zero; electric field lines intersect the particle surface perpendicularly (see fig. 1a). Since the particle is suspended in an electrolyte, ions in solution are driven by the field and accumulate at the electrolyte/particle interface, inducing an EDL. Diffusion opposes this counter-ion attraction to the interface, and the characteristic charge cloud at which the two forces balance defines the diffuse layer. If the electric field is high enough, electrons can jump from the conducting particle to the molecules in the liquid or vice versa leading to redox reactions. In the following analysis, we assume that the induced voltage across the double layer $\Delta\phi \sim E\ell$ (where E is applied electric field and ℓ is typical particle size) is below the threshold voltage for these Faradaic reactions V_{redox} so that no direct current passes through the EDL, i.e. the electrolyte/conductor interface is perfectly polarizable. When steady state is reached, the EDL induced charge is maximum, there are no normal currents at the interface and the field lines surround the particle (see fig. 1b). Typical values for a threshold voltage for Faradaic reactions V_{redox} can be around 1

volt. For example, mercury in contact with a deaerated KCl solution behaves as a perfectly polarizable interface over a potential range of about 2 volts [21]. The typical time for charging the electrolyte/metal interface is $t_{RC} = \varepsilon\ell/\lambda_D\sigma$ [22, 23], where ε and σ are, respectively, the electrical permittivity and conductivity of the electrolyte, and λ_D is the Debye length. This time can be viewed as the RC time for charging the EDL capacitance through the resistance of the bulk electrolyte $t_{RC} = C_{DL}\ell/\sigma$ with $C_{DL} = \varepsilon/\lambda_D$ the EDL capacitance (per unit area) using the Debye-Huckel approximation. When an AC field is applied, then for frequencies of applied signal much higher than the reciprocal of the charging time ($f \gg f_{RC} \equiv 2\pi/t_{RC}$), the induced EDL charge is negligible, field lines intersect the particle surface perpendicularly, and the situation is equivalent to a conductor in a dielectric (see fig. 1a). For applied frequencies much lower than $2\pi/t_{RC}$, there is enough time for the EDL to fully charge and the electric field lines surround the particle. From the perspective of an observer, the situation is equivalent to that of an insulating particle (see fig. 1b).

In figure 1 we have assumed that particle surface conduction is negligible compared to electrolyte bulk conduction. In other words, the particle has a low Dukhin number [24], where the Dukhin number is given by $\sigma_s/\sigma\ell$, with σ_s the particle surface conductivity. This number can be high for metal nanocolloids ($\ell \ll 1\,\mu$m), which are usually highly charged in order to form stable suspensions. In this case, the native double layer may contribute to surface conductance implying a high Dukhin number, which can lead to concentration polarization phenomena [24]. In this paper, we will only deal with small Dukhin numbers and/or negligible intrinsic charge.

1.2. Induced motion of a conducting particle

The electrically induced motion of an uncharged conducting particle in an electrolyte arises from the interaction of the electric field with the induced dipole of the particle plus its double layer, together with the viscous stresses of the induced electrokinetic flow around the particle, a combination of effects called dipolophoresis by Shilov and co-workers [25, 26]. Typical particle motions aris-

ing from the interaction of the field with the induced dipole are [1, 2, 27]: dielectrophoresis (DEP), when the particle moves in a non-uniform field; electrorotation (ROT), when the particle rotates due to a rotating field; and electroorientation (EOr), when a non-spherical particle orients in a homogeneous field. These dipole-induced motions are well understood theoretically and well documented experimentally, mainly when double-layer (electrokinetic) effects are not important. The electrokinetic flow due to the action of the applied field on the induced EDL charge has been called "induced-charge electroosmosis" (ICEO) and the particle motion due to this flow "induced-charge electrophoresis" (ICEP) [28]. Early studies of the physical origin of this electrokinetic flow have been discussed, for example, in refs [29–31]. Early observations of ICEO flow around a metal sphere were reported by Gamayunov et al [32]. Experimental and theoretical studies of ICEO around microelectrodes or metal objects have been widely reported [22, 28, 33–41] and ICEP of polarizable particles [42–48] has attracted increasing attention from the microfluidics and lab-on-chip community [49], see the review about induced-charge electroosmosis and electrophoresis by Bazant and Squires [50]. ICEO flow around a particle is generally important at low frequencies, from DC up to frequencies of the order of $\omega_{RC} = 1/t_{RC}$, while the force on the dipole is generally important at all frequencies.

This review is organized as follows. We describe the theory for small applied voltages and thin double layers and show how the dynamics of the particle is obtained from the electrical forces and fluid flows. We continue with a review of experimental results reporting translation or rotation of metal particles. The experiments are quantitatively compared with the theoretical predictions of the previous section. Finally, we include a section on the assembly of particles on the surface of microelectrodes or between them, and self-assembly induced by electric fields. Among the many applications, assembly has attracted considerable interest and, therefore, the understanding of the AC electrokinetic behaviour is fundamental if the assembly process is to be controlled. Finally, the main

results are summarised together with discussions on possible future directions.

2. Mathematical formulation for small voltage and thin double layer

We assume that the typical induced particle velocity is small enough so that convection of charge is negligible. In this situation, the charge distribution is not affected by the motion of the particle. The electrical equations can be solved independently with the solution then inserted into the mechanical problem. The weak field approximation ($E\ell \ll k_B T/e$) guarantees that charge convection is negligible [40, 46, 47].

Electrical problem. The amplitude of the AC electric potential is small enough so that the bulk salt concentration is unperturbed. At scales much larger than the Debye length the electrolyte remains electroneutral and the electric potential satisfies Laplace's equation in the liquid bulk,

$$\nabla^2 \phi = 0 \tag{1}$$

The corresponding boundary condition at the polarizable particle surface reflects the charging of the double layer by the current in the bulk

$$\sigma \frac{\partial \phi}{\partial n} = C_{DL} \frac{\partial \Delta\phi}{\partial t} \tag{2}$$

where the unit normal points outwards, the normal derivative is computed at the outer boundary of the EDL, and $\Delta\phi = \phi - V$ is the difference between the potential just outside the double layer and the potential in the conductor V. Here we have assumed that the signal frequency is much smaller than the charge relaxation frequency $\omega \ll \sigma/\varepsilon$ in order that the diffuse layer can be considered to be in quasi-equilibrium [51].

Mechanical problem. The Reynolds number is small so that the velocity field satisfies Stokes' equations

$$\eta \nabla^2 \mathbf{u} = \nabla p \qquad \nabla \cdot \mathbf{u} = 0 \tag{3}$$

where η is the dynamic viscosity of the liquid. The boundary condition at the particle surface (including its EDL) is $\mathbf{u} = \mathbf{U} + \Omega \times \mathbf{r} + \mathbf{u}_{HS}$, where $\mathbf{U}$ is the translational velocity of the particle center of reaction, $\mathbf{\Omega}$ is the particle angular velocity, and $\mathbf{u}_{HS}$ is the Helmholtz-Smoluchowski slip velocity. For a thin double layer in quasi-equilibrium, on a perfectly polarizable metal surface, this is given by $\mathbf{u}_{HS} = -(\varepsilon/\eta)\zeta\mathbf{E}_s$ [29], where ζ is the potential drop from the "slip plane" to the bulk electrolyte (just outside the EDL) [52] and $\mathbf{E}_s$ is the tangential electric field just outside the EDL. Here we are interested in the time-averaged velocity,

$$\mathbf{u}_{HS} = -\langle\frac{\varepsilon}{\eta}\zeta\mathbf{E}_s\rangle = \langle\frac{\varepsilon}{\eta}\Lambda\Delta\phi\mathbf{E}_s\rangle \tag{4}$$

where $\langle\dots\rangle$ stands for time average, and Λ is a parameter that relates the induced ζ-potential to the total EDL voltage $\Delta\phi$. For the ideal case where all the EDL voltage contributes to the slip velocity $\Lambda = 1$. Experimental observations show that the slip velocity is usually smaller than the ideal case ($\Lambda < 1$) and sometimes very much smaller [53]. For a metal surface the slip velocity can also be written as $\mathbf{u}_{HS} = -(\varepsilon/2\eta)\Lambda\langle\nabla_s(\Delta\phi)^2\rangle$, where ∇_s is the tangential gradient operator, taking into account that V is constant. Several reasons have been proposed for the reduction of the slip velocity from the ideal case of $\Lambda = 1$ including dielectric coating [37, 54], ion adsorption [54, 55], counterion crowding [53], surface roughness [56], surface conduction [57], residual Faradaic reactions [58, 59] and/or flow instability of the concentration polarization layer [60]. Experimentally, the ICEO slip velocity tends to decrease with electrolyte conductivity and is usually negligible for conductivity of the order of 0.1 S/m and above.

The translational and rotational velocities are determined by imposing equilibrium of forces and torques. It is convenient to decompose the velocity field as the sum of the flow generated by a translating and rotating particle and a flow generated by the slip velocity on a stationary particle. In this way, the equilibrium of forces and torques can be written, respectively, as

$$\eta\mathbb{M}\cdot\mathbf{U} + \eta\mathbb{C}\cdot\mathbf{\Omega} = \langle(\mathbf{p}\cdot\nabla)\mathbf{E}\rangle + \int_{S_p}\mathbb{T}_{\mathrm{H}}\cdot\mathrm{d}\mathbf{S} \tag{5}$$

$$\eta\mathbb{C}\cdot\mathbf{U}+\eta\mathbb{N}\cdot\mathbf{\Omega}=\langle\mathbf{p}\times\mathbf{E}\rangle+\int_{S_p}\mathbf{r}\times\mathbb{T}_{\mathrm{H}}\cdot\mathrm{d}\mathbf{S} \tag{6}$$

where $\mathbb{T}_{\mathrm{H}}$ is the hydrodynamic stress tensor for the velocity field which comes from the slip velocity on a stationary particle, and S_p is a surface that encloses the particle together with its double layer. Here $\mathbb{M}$, $\mathbb{N}$ and $\mathbb{C}$ are, respectively the translation, rotation and coupling tensors [61]. For arbitrary particles translational and rotational motions are coupled, as for example, screw-like particles. In this paper, we mainly deal with particles with sufficient symmetry (orthotropic bodies) so that the coupling tensor is zero, $\mathbb{C}=0$. In this situation, solving for $\mathbf{U}$ in eq. 5 and $\mathbf{\Omega}$ in eq. 6, we can write $\mathbf{U}=\mathbf{U}_{DEP}+\mathbf{U}_{ICEP}$ with

$$\mathbf{U}_{DEP}=\eta^{-1}\mathbb{M}^{-1}\cdot\langle(\mathbf{p}\cdot\nabla)\mathbf{E}\rangle\qquad\mathbf{U}_{ICEP}=\eta^{-1}\mathbb{M}^{-1}\cdot\int_{S_p}\mathbb{T}_{\mathrm{H}}\cdot\mathrm{d}\mathbf{S} \tag{7}$$

and $\mathbf{\Omega}=\mathbf{\Omega}_{DEP}+\mathbf{\Omega}_{ICEP}$ with

$$\mathbf{\Omega}_{DEP}=\eta^{-1}\mathbb{N}^{-1}\cdot\langle\mathbf{p}\times\mathbf{E}\rangle\qquad\mathbf{\Omega}_{ICEP}=\eta^{-1}\mathbb{N}^{-1}\cdot\int_{S_p}\mathbf{r}\times\mathbb{T}_{\mathrm{H}}\cdot\mathrm{d}\mathbf{S} \tag{8}$$

Here the subscripts DEP and ICEP refer respectively, to particle motion induced by a DEP force or by an ICEO flow around the particle. By way of example, consider a sphere of radius a subjected to an electric field. In the thin double layer approximation, we have:

$$\mathbf{U}_{DEP}=\frac{\langle(\mathbf{p}\cdot\nabla)\mathbf{E}\rangle}{6\pi a\eta}\qquad\mathbf{U}_{ICEP}=-\frac{1}{4\pi a^2}\int_{S_p}\mathbf{u}_{HS}dS \tag{9}$$

$$\mathbf{\Omega}_{DEP}=\frac{\langle\mathbf{p}\times\mathbf{E}\rangle}{8\pi a^3\eta}\qquad\mathbf{\Omega}_{ICEP}=-\frac{3}{8\pi a^3}\int_{S_p}\mathbf{n}\times\mathbf{u}_{HS}dS \tag{10}$$

where the translation U_{ICEP} and angular Ω_{ICEP} velocities are expressed as certain integrals of the slip velocity $\mathbf{u}_{HS}$ on the particle surface thanks to the Lorentz reciprocal theorem [62].

3. Induced translational motion

In electrophoresis charged particles move in a fluid due to the action of a spatially uniform electric field [63]. In general, using AC electric fields, particles

undergo translational motion if the electric field is inhomogeneous. If the electric field is homogeneous, particles can move by ICEP if they are asymmetric, but only using low frequency AC fields. For high-frequency fields ($\omega \gg \omega_{RC}$) the translational motion is only due to the force on the dipole, $(\mathbf{p} \cdot \nabla)\mathbf{E}$, and this force is zero in homogeneous fields.

3.1. Uniform field

At low frequencies, including DC, the induced flow around an asymmetric particle can produce particle motion [42]. Breaking the geometric symmetry of the ICEO flow around a conducting object generally leads to net pumping of fluid past the object, which for a suspended microparticle leads to translation. An asymmetric particle can be constructed from a symmetrically shaped one but with inhomogeneous surface properties, or it can be an asymmetric body. This idea was experimentally demonstrated using Janus spherical particles [45]. The Janus particles were polystyrene micro-spheres with one half coated with gold. Under the action of the applied field, the particles orient with their equatorial plane separating the dielectric and metal hemispheres parallel to the electric field. This rotation is a combination of dipole induced rotation plus ICEO induced rotation. The particle then moves perpendicularly to the electric field lines, advancing in the direction of the non-conducting dielectric end. This is because ICEO flow occurs only on the metal hemisphere (see Figure 2). Particles diameters were between 4 and 9 microns in ref. [45], and equal to 50 microns in ref. [64]. For these diameters we do not expect high Dukhin numbers due to native charge. At very low frequencies and assuming negligible Dukhin number, the electric field lines surround the particle and the potential is of the form

$$\phi = -E_0 \cos\theta \left(r + \frac{a^3}{2r^2} \right) \tag{11}$$

The slip velocity is then $\mathbf{u}_{HS} = \Lambda(9\varepsilon E_{rms}^2 a/4\eta)\cos\theta \sin\theta \mathbf{e}_\theta$ on the metal side and zero on the dielectric side. From eq. 9, the velocity acquired by the particle is $\mathbf{U}_{ICEP} = \Lambda(9/64)(\varepsilon E_{rms}^2 a/\eta)\mathbf{e}_y$, where $\mathbf{e}_y$ points towards the dielectric hemisphere of the particle [42, 45]. The experimentally determined particle

motion was in semiquantitative agreement with theory for low electrolyte concentrations. The induced velocity was about an order of magnitude smaller than predicted with $\Lambda = 1$ and decreased for increasing saline concentration. For saline (NaCl) concentrations greater than approximately 10 mM, no particle motion was observed.

3.2. Non-uniform field

We begin by analysing the case of a conducting sphere subjected to a non-uniform electric field. Here we follow reference [42], adapting the analysis to AC fields. The applied electric field is of the form $\mathbf{E} = \mathbf{E}_0 + \mathbb{G} \cdot \mathbf{r}$, where $\mathbb{G}$ is a symmetric matrix that defines the gradient of the field, and the periodic variation in time is assumed. Phase shift between $\mathbf{E}_0$ and $\mathbb{G}$ is not considered, i.e. both are real. The total electric potential results from the applied potential plus the induced potential due to an induced dipole and induced quadrupole:

$$\phi = -\mathbf{E}_0 \cdot \mathbf{r} - \frac{1}{2}\mathbf{r} \cdot \mathbb{G} \cdot \mathbf{r} + \alpha \frac{\mathbf{E}_0 \cdot \mathbf{r}}{r^3} + \frac{\beta}{2}\frac{\mathbf{r} \cdot \mathbb{G} \cdot \mathbf{r}}{r^5} \tag{12}$$

The complex constants α and β are determined by the boundary condition of double layer charging at the surface of the particle which is, in phasor notation,

$$\frac{\partial \phi}{\partial r} = \frac{i\bar{\omega}}{a}\phi \tag{13}$$

where $\bar{\omega} = \omega C_{DL} a/\sigma$ is nondimensional. The constants are

$$\alpha = \frac{-1 + i\bar{\omega}}{2 + i\bar{\omega}} a^3 \qquad \beta = \frac{-2 + i\bar{\omega}}{3 + i\bar{\omega}} a^5 \tag{14}$$

With the expression for the potential, the ICEP velocity can be obtained [42]

$$\mathbf{U}_{ICEP} = \frac{1}{4\pi a^2} \int \frac{\Lambda\varepsilon}{2\eta} \mathrm{Re}\left[\phi \nabla_s \phi^*\right] dS = \frac{\Lambda\varepsilon a^2}{\eta} \mathrm{Re}[c_1 c_2^*] \mathbb{G} \cdot \mathbf{E}_0 \tag{15}$$

where $c_1 = (2 + i\bar{\omega})^{-1}$ and $c_2 = (3 + i\bar{\omega})^{-1}$. The expression can be written in terms of $\nabla|\mathbf{E}|^2$ at $r = 0$, since $\nabla|\mathbf{E}|^2 = 2\mathbb{G} \cdot \mathbf{E}_0$, leading to

$$\mathbf{U}_{ICEP} = \frac{\Lambda\varepsilon a^2}{2\eta} \frac{6 + \bar{\omega}^2}{(6 + \bar{\omega}^2)^2 + \bar{\omega}^2} \nabla|\mathbf{E}|^2 \tag{16}$$

The ICEP velocity decreases for increasing $\bar{\omega}$ and is maximum at $\bar{\omega} = 0$ with a value of $\mathbf{U}_{ICEO} = \Lambda(\varepsilon/12\eta) a^2 \nabla|\mathbf{E}|^2$. The expression is identical to that given

in ref. [42], taking into account that time-average of $\cos^2(\omega t)$ is equal to 1/2. The motion induced by the force on the dipole $\mathbf{p} = 4\pi\varepsilon\alpha\mathbf{E}_0$ is

$$\mathbf{U}_{DEP} = \frac{1}{12\pi a\eta}\mathrm{Re}[(\mathbf{p}\cdot\nabla)\mathbf{E}^*] = \frac{\varepsilon a^2}{6\eta}\frac{(\bar{\omega}^2-2)}{(\bar{\omega}^2+4)}\nabla|\mathbf{E}|^2 \tag{17}$$

$\mathbf{U}_{DEP}$ changes sign with $\bar{\omega}$: it is negative at low frequencies and positive at high frequencies. Interestingly, it is predicted that the DEP and ICEP velocities at low frequencies are opposite and cancel out for $\bar{\omega} = 0$ and $\Lambda = 1$ [26, 42, 48]. This cancelation has not been observed experimentally. Mainly, the observed translational motion of conducting spheres was explained by the action of the field on the induced dipole [19, 65]. In these experiments, polystyrene microspheres were coated with nanocolloidal gold. The Au-coated microparticles were slightly heavier than water and sedimented so that the observed motion was for particles confined to the bottom wall of the sample cell. Figure 3a shows real and imaginary parts of nondimensional polarizability $\bar{\alpha} = (-1+i\bar{\omega})/(2+i\bar{\omega})$ for a conducting sphere as a function of nondimensional frequency $\bar{\omega}$. The experimental DEP velocities follow the same trend as the real part of $\bar{\alpha}$ (fig. 3c). Particles move away from high fields (negative DEP) at low frequencies and towards high fields (positive DEP) at high frequencies. The influence of ICEP was negligible. This is not entirely surprising since experimentally the induced charge electroosmotic flow is smaller than predicted for an ideal double layer as already discussed above. In addition, these spheres had rough surfaces, because of the way the gold coating was made, which reduces the ICEO flow [56]. Other researchers have measured positive DEP of conducting micron and submicron particles at high frequencies [15]. The low frequency DEP behavior is difficult to observe experimentally because of the appearance of AC electroosmotic (ACEO) flow near the electrodes which tends to mask the observations [15, 66]. Experiments on the DEP behaviour of particles positioned in the center of four co-planar electrodes avoids much of this problem (see fig. 3b) since near the center the ACEO flow is very small [19, 65]. In addition, accurate measurements of the translational motion was aided by using Au-coated latex particles with almost neutral density which reduces the solid friction with substrate [19, 65].

The literature on dielectrophoretic assembly of metal nanocolloids reported only positive DEP [4, 67]. The gold nanoparticles had diameters of 5, 15 and 20 nm [4], so that the Debye length in DI water would be greater than 20 nm. In this case, the thin double-layer approximation is not valid and thick double-layer theory should be used instead [48]. This theory predicts that the translational motion is towards high electric fields for all frequencies, i.e. equivalent to positive DEP, and that the motion is mainly due to ICEP at low frequencies and DEP at high frequencies. According to theory, the DEP contribution is negative at low frequencies, although ICEP dominates. However, the theory is for uncharged particles and gold nanoparticles are highly charged in order that they form stable suspensions. In this case the Dukhin number is likely to be high [24] and therefore particles may have a positive dipole at low frequencies as well. The observations of different particle assembly behaviour for different frequencies was attributed to different forces on the suspending electrolyte (AC electroosmosis and electrothermal flows) [4]. Nanoparticle capture was observed over the entire tested frequency range (10Hz to 1 MHz), indicating positive DEP.

When a nonuniform electric field is applied to a metal rod, it first tends to align with the electric field and then moves to regions of high field. Depending on frequency, this attraction should mostly be due to ICEO around the particle at low frequencies or to the force on the dipole at the high frequency range. For a polarizable rod, the induced dipole at low frequencies is very small since the electric field lines surround the rod almost without deviation (see fig. 1b). Therefore, the DEP force at low frequencies is negligible compared to the DEP force at high frequencies. The transition frequency is of the order of $\omega_{RC} = \sigma/C_{DL}b\ln(a/b)$, where a and b are, respectively, the rod semi-length and rod radius [20]. The main experimental observation concerning the translational motion of metal rods is that they move to high field regions [16, 68, 69]. Some authors observe changes in the dielectrophoretic force with frequency in the MHz region [68], which is well above ω_{RC}. This behavior cannot be attributed to changes in the polarizability of the metal rod, which must be constant up to very high frequencies. In this respect, the theoretical pre-

diction of DEP force decrement due to Maxwell-Wagner (MW) polarization for frequencies beyond 10^5 Hz in [16] is based upon a wrong approximation. The MW frequency for a leaky dielectric slender spheroid in a leaky dielectric liquid is approximately $\omega_{MW} \approx (\sigma_f + \sigma_p L)/(\varepsilon_f + \varepsilon_p L)$, where subscripts f and p refer to the fluid and particle, respectively, and L is the depolarization factor along the particle axis [1]. For a metal rod and for typical rod slenderness ($\sigma_p L \gg \sigma_f$), the MW relaxation frequency in water is beyond 10^{12} Hz, clearly outside the quasi-electrostatic limit. Very recently, the Maxwell-Wagner frequency has been used in electro-orientation experiments for the determination of conductivities of semiconducting nanorods [70].

4. Induced rotational motion

In this section we describe results where rotation of a conducting particle occurs upon application of an AC field. Two cases are distinguished: alignment of a non-spherical particle in an AC field with fixed direction, called electro-orientation; and the continuous rotation of a particle subjected to a rotating electric field, called electro-rotation. In both cases, the particle angular velocity is usually much smaller than the frequency of the AC field. Electro-orientation (electro-rotation) results from the interaction of the applied field with the in-phase (out-of-phase) induced charge, which means that the frequency dependence of EOr (ROT) mirrors the real (imaginary) part of the particle polarizability. In both cases, we analyse rotation due to the electrical torque on the induced dipole and rotation due to the ICEO flow at the metal-electrolyte interface.

4.1. Unidirectional field

When exposed to an applied field, slender metal particles (e.g. rods) tend to align with the applied electric field for all frequencies. However, the motion is mainly induced by ICEO flow around the particle at low frequencies and by the torque on the induced dipole at high frequencies [20, 71]. The characteristic frequency of transition is of the order of $\omega_{RC} = \sigma/C_{DL} b \ln(a/b)$. At low

frequencies, perfectly polarizable slender particles almost do not perturb the electric field lines, meaning that the induced dipole is very small. At these frequencies, the rotational motion that is observed for slender particles is due to ICEP [43, 44]. The expression for the ICEP rotational velocity for slender particles at low frequencies is $\Omega_{ICEP} = (\varepsilon/2\eta)\Lambda E_0^2 \cos\theta \sin\theta$. As the frequency increases the ICEO flow disappears, but the induced dipole increases reaching a plateau. At high frequencies, the torque on the induced dipole aligns the particle with the electric field and the DEP angular velocity for slender particles is $\Omega_{DEP} = (\varepsilon/4\eta)E_0^2 \cos\theta \sin\theta$. Adding both contributions, the frequency dependence of the angular velocity is of the form [20]

$$\Omega = \left(\frac{\Lambda}{1+\bar{\omega}^2} + \frac{\bar{\omega}^2}{2(1+\bar{\omega}^2)} \right) \frac{\varepsilon}{2\eta} E_0^2 \cos\theta \sin\theta \tag{18}$$

where $\bar{\omega} = \omega/\omega_{RC}$. The ICEP orientation of a nanowire can be qualitatively understood according to the schematic diagrams in Figure 4a which shows a metal nanowire subjected to an electric field of arbitrary direction [20]. The axial component of the electric field induces charges in the diffuse layer and ICEP rotation is generated by the action of the perpendicular component of the electric field. The situation is analogous to considering the upper part of the rod as a particle undergoing electrophoretic motion to the right, while the lower part is akin to a particle undergoing electrophoresis to the left. At high frequencies, ICEP rotation is negligible and the nanowire behaves as a conductor suspended in a dielectric (see fig. 1a). The induced dipole is maximum and the applied torque orients the nanowire.

The observation that metal nanowires align with its main axis parallel to the applied electric field direction has been extensively reported [12, 17, 68], idem for carbon nanotubes [72]. Experimental observations of the electrical orientation of metal rods at low frequencies show that they align with the electric field due to ICEP [73, 74]. The fact that ICEO flow around conducting rods is happening at low frequencies can be inferred from the observed hydrodynamic interaction between pairs of rods at these frequencies [20, 74]. Experiments that

compare electrical orientation at low and high frequency clearly show that the orientation is stronger at high frequencies [20, 75]. Figure 4b) shows the electro-orientation spectrum for silver nanowires with lengths between 6 and 7 microns and aspect ratios around 0.04 [20]. The figure shows a plot of the orientation rate versus the frequency of the AC signal (nondimensional). Experimental data for three different electrolyte conductivities are shown and the continuous line is the prediction for the EOr motion generated by the electrical torque. For high frequencies, experimental data are below the theoretical prediction, most probably due to wall effects [75, 76]. Interestingly, for low frequencies the DEP torque predicts negligible EOr. As mentioned above, orientation is due to ICEP in this case, although for the ideal case $\Lambda = 1$ the prediction is much higher. EOr experiments with conducting carbon nanotubes (CNTs) suspended in Laromer-solvent mixtures of different conductivities also showed smaller orientation at low frequencies than at high frequencies [72], with a transition frequency given by the reciprocal of the RC time for charging the EDL around the particle. These CNTs were good conductors since they had electrical conductivities much greater than the Laromer-solvent mixture.

In order to measure the electro-orientation of conducting nanowires two approaches have been pursued in the literature: measurement of the angular speed [20, 72], and measurement of the degree of electrical alignment of nanowires in competition with thermal (Brownian) forces [72, 73, 75]. The latter experimental technique requires lower voltages compared to the deterministic experiments. This is particularly useful when the goal is to compare experiments with electrokinetic theories, which are mainly developed for small voltage drops across the EDL ($\Delta\phi < k_B T/e \approx 25$ mV). Another important benefit of these experiments is that electrokinetic torques are determined independently of the rotational friction coefficient, a parameter that is difficult to measure accurately.

As already mentioned, Janus spheres orient with their equatorial planes parallel to the electric field direction [45] due to a combination of ICEP and DEP rotation. Interestingly, continuous rotation in a unidirectional field is possible for assemblies of Janus spheres due to ICEP, as predicted in ref [42] (ever-

rotating structures). It was shown that an assembly of three Janus particles will rotate as a consequence of the individual ICEP motion of each Janus particle. This rotation can also happen with two Janus spheres, as observed in [77] (see Figure 4c)). In these experiments, the composite particles rotated and translated on a substrate and the unidirectional field was applied perpendicularly to the substrate. The Janus spheres have about 5 micron diameter. The motion can be understood qualitatively from the tendency of Janus particles to move perpendicularly to the electric field towards the dielectric side in ICEP.

4.2. Rotating field

For a rotating electric field the torque on the induced dipole of the sphere is $\langle N\rangle = -4\pi\varepsilon \mathrm{Im}[\alpha]E_0^2$, where $\alpha = a^3(-1+i\bar{\omega})/(2+i\bar{\omega})$ for a perfectly polarizable sphere (eq. 14). Therefore, taking into account the viscous torque on a rotating sphere, the angular velocity is

$$\Omega_{DEP} = -\frac{\varepsilon}{2\eta}\frac{3\bar{\omega}}{4+\bar{\omega}^2}E_0^2 \tag{19}$$

with a maximum at $\bar{\omega} = 2$ equal to $|\Omega_{max}| = 3\varepsilon E_0^2/8\eta$. From symmetry, the ICEO slip velocity on a conducting sphere does not produce rotation and, therefore, the sphere angular velocity is $\Omega = \Omega_{DEP}$ [65, 78]. ROT experiments with metal spheres showed counter-field rotation and the angular velocity as a function of frequency showed a single peak at the characteristic RC frequency for charging the EDL [19, 65, 79]. The maximum angular velocity is close to prediction (within an error smaller than 20%) when the effect of the wall on the viscous and electrical torques is taken into account [65, 79]. A measurement of the frequency for maximum angular rotation provides a means for measuring the capacitance of the double layer. It was observed that for spheres with rough surface the capacitance was greater than that predicted by the Debye-Huckel theory ε/λ_D [65], but for Ti spheres with smooth surfaces the capacitance was approximately close ($C_{DL} \sim \varepsilon/\lambda_D$) [79]. The experiments were made using spheres with diameters ranging between 10 and 45 microns, much greater than the Debye length of the electrolyte (around 30 nm or less) so that the thin

double layer approximation was valid. Recently, theoretical work on the ROT of metal spheres with arbitrary Debye length [78] shows that not only the electrical torque, but also ICEP rotation has to be considered. While the former generates counter-field rotation, the latter generates co-field rotation. It is found that for very thick double layers the two contributions compensate each other and no net particle rotation is expected.

According to theory [20, 71], when subjected to a rotating field, slender conducting particles rotate due to ICEO flow around the particle and to the torque on the induced dipole. The ICEP rotation is co-field while the DEP rotation is counter-field and both behaviors exhibit a single maximum at the angular frequency given by $\omega_{RC} \sim \sigma/C_{DL}b\ln(a/b)$. Both mechanisms result from the interaction of the out-of-phase induced charge with the applied electric field. For very slender particles, the theoretical ROT angular velocity is

$$\Omega = (2\Lambda - 1)\frac{\varepsilon E_0^2}{4\eta}\frac{\omega/\omega_{RC}}{1+(\omega/\omega_{RC})^2} \tag{20}$$

ROT experiments with metal rods have been reported [11, 80] and the angular velocity as a function of frequency showed a single peak. ROT experiments using Ag nanowires [80] show counterfield rotation that closely matches dipole theory (see fig. 4d), indicating that ICEP rotation is again much smaller than expected for an ideal double layer ($\Lambda \ll 1$). The measured frequencies of maximum rotation were close to the reciprocal of the RC time for charging the EDL around the metal particle ω_{RC}. These experimentally measured Ag nanowires were suspended in KCl aqueous solution with conductivity ranging between 1.5 mS/m and 15 mS/m. Figure 4d shows the rotation speed as a function of non-dimensional frequency. The continuous line is a prediction of the velocity of rotation obtained from the electrical torque. The EDL capacitance values were obtained from the frequency of maximum rotation and, interestingly, experimental values were close to those predicted by the Debye-Huckel theory $C_{DL} = \varepsilon/\lambda_D$ (probably because the induced EDL voltages are small). Part of the deviation between dipole theory and experiments could also be attributed to the effect of the wall [76].

5. Electric-field induced assembly of metal particles

In previous sections we focused on the electrical manipulation of a single metal particle immersed in a electrolyte. Several publications also describe the behaviour of a collection of metal particles subjected to AC fields. In this case, both electrical and hydrodynamic particle-particle interactions occur upon application of an electric field. These interactions usually lead to reconfigurable particle patterns with potential applications in microelectronics and sensing. In the following section we review experiments on the assembly of metal particles.

5.1. Metal particle assembly on microelectrode structures

Electric fields in microdevices are usually generated using planar microelectrode structures fabricated on glass or other insulating substrates. Several publications describe experiments where metal nanocolloids dispersed in an electrolyte move towards electrodes and thereby accumulate. This motion of metal particles could be due to positive DEP at high frequencies, as described in section 3.2, and/or by fluid flow induced on the electrodes at low frequencies, such as AC electroosmosis [22]. For example, reference [3] shows that the dielectrophoresis of metal colloids can lead to the formation of microwires in the gaps of planar electrodes, see figure 5a. This assembly is proposed as a quick method to realize electrical connections to conductive islands or particles, as shown in ref. [3] by a clear and abrupt change in the electrical current through the cell. Since then, several works have extensively reported the use of metal nanoparticles for bridging electrodes [81–88]. The influence of signal frequency on the metal nanoparticle assembly in small gaps between electrodes was studied in ref.[4], see figure 5b. It was shown that particle motion by ac electroosmosis greatly influences the morphology of resultant nanoparticle assemblies.

A different approach to perform nanocontacts between electrodes is the use of a single metal nanowire. For example, AC electric fields are used to bring and place a nanowire between microelectrodes [10, 89], see figure 5c. Bridging of

larger gaps between electrodes has also been reported by the dielectrophoretic assembly of several metallic nanowires [69] or carbon nanotubes [90], see figure 5d. Electrical manipulation of metal nanowires has also been applied for the fabrication of nanoelectromechanical resonators by assembling nanowires on electrodes, as reported in [91]. A recent review on the assembly of nanostructures using electric fields can be found in ref. [92].

5.2. Chaining and self assembly of metal particles

As previously mentioned, particle-particle interactions occur upon application of an electric field to an aqueous dispersion of metal particles. One of these interactions is of electrical nature and has its origin in the polarization of the particles. The force between particles can be described via dipole-dipole interactions and higher-order multipoles [1]. The effects can be qualitatively understood by considering the electrical dipoles induced on neighboring particles. For example, consider two metal spheres immersed in an electrolyte and subjected to an homogeneous electric field. Attraction or repulsion between spheres depends on the relative alignment of the two spheres with respect to the electric field direction. As schematically depicted in figure 6a, if the particles are oriented with their line of centers parallel to the applied field, the interaction between induced dipoles is attractive irrespective of the signal frequency. On the other hand, if the particles alignment is perpendicular to the field, the induced dipoles repel. Dipole-dipole attraction explains the ubiquous observation of chains of metal particles along the direction of the electric fields, a phenomenon commonly known as *pearl chaining* [1] (see for example the chains in figure 5). Also, dipole-dipole interactions explain the formation of chains of metallodielectric Janus spheres under an ambient AC field [5, 93] (see Figure 6b). Interestingly, by using controlled patchy metallodielectric spheres, complex microstructures can be assembled by applying high frequency fields [6].

Chaining of metal nanowires has also been observed at high frequencies [14] (see fig. 6d). For low frequencies, assembly into a different pattern was ob-

served (see fig. 6c). In this case the nanowires orient parallel to the field, but form bands perpendicular to the direction of the electric field. This pattern seems to be driven by the hydrodynamic interaction between particles that arises from the ICEO flow around the nanowires. As observed in ref. [74], when two nanowires are close they first align end-to-end, then slide next to one another, and finally move apart from their centers. The wavy bands result because the particles remain within a distance of a few microns, but the reason for this equilibrium position is not clear at present. In all cases, the assembly is reversible and takes a few seconds to reach equilibrium. The formation of bands takes longer for increasing conductivity of the electrolyte [14]. This result is in agreement with the general observation of decreasing ICEO velocities for increasing electrolyte conductivity. Electrokinetic fabrication of vertically aligned carbon-nanotube/polymer composites has been reported using electro-orientation at low frequencies so that the ICEO flow favored individually aligned CNTs rather than tip-to-tip chaining [72].

6. Conclusions and outlook

Electrical forces on conducting particles can lead to linear motion, rotation and orientation, which can be used for particle alignment, separation and assembly. Critical to exploiting these forces is a thorough understanding of the fundamental principles and effects. Several experimental observations have recently shown the potential for using AC electric fields to precisely manipulate metal microspheres and metallic and semiconducting nanowires dispersed in aqueous electrolytes. Controlled assembly onto or between microelectrodes and self-assembly induced by AC electric fields have been demonstrated by several groups. Particle dynamics can be explained from the action of the applied field on the charges induced within the EDL. Theoretical work shows how to model this action, and experimental results demonstrate that the particle motion can be predicted from the action of the electrical forces on the particle plus a contribution due to the ICEO flow around it. The observed translational motion

of metal spheres in non-uniform fields is explained by the force on the induced dipole (DEP), with negligible ICEP. The translational motion of Janus spheres in uniform fields is only possible due to ICEP, and observed particle velocities are smaller than for the ideal case. According to theory, the ROT of spheres is only affected by the electrical torque on the dipole, and experiments are in close agreement with theory. However, the theoretical analysis for the ROT of nanowires predicts some influence of ICEP rotation. This influence could not be observed in experiments, which showed that ROT of nanowires could be explained by the torque on the induced dipole. Electro-orientation theory predicts that conducting nanowires should align with the applied field for all applied frequencies. At low frequencies the electrical torque vanishes and the orientation is due to ICEP, while at high frequencies the ICEP vanishes and EOr occurs because of the electrical torque. Both mechanisms have been experimentally demonstrated. Understanding the behaviour of metal nanowires is a very interesting problem because ROT experiments provide a precise measurement of the characteristic frequency ω_{RC}, while EOr allows experimental separation of the two contributions, providing a relative measure of the two mechanisms.

For simplicity, the theoretical analysis has dealt with particles with thin double layers. Theoretical work for arbitrary Debye length has been reported and experimental validation of these predictions is required. These results will shed light on the fundamental problem of induced-charge electrokinetics and the induced zeta potential. Future work could focus on an improved analysis of the effect of the wall on both the electrical and hydrodynamic problems.

ICEP velocities in experiments are often one order of magnitude smaller than predicted by the simplest theory. An arbitrary constant Λ is used to account for this discrepancy. Experiments with metal particles should shed light on the reasons of these discrepancies. From a fundamental perspective, the AC electrokinetics of conducting particles is a problem where the particle velocity is measured for a known EDL potential. This implies that the zeta potential can be measured for a controlled voltage drop across the double layer.

Finally, particle-particle interactions give rise to a rich complexity that de-

mands further study. These phenomena could be interesting not only for fundamental reasons but for application in the control of reversible particle self-assembly. Future work could lead to bottom-up methods for assembling a diverse range of nano-systems from simple building blocks. Exploiting electric and hydrodynamic particle-particle interactions could be used for programmable assembly or synthesis of large nano-scale structures.

Acknowledgements

We acknowledge financial support from Spanish Government Ministry MEC under contract No. FIS2014-54539-P.

References

[1] T. Jones, Electromechanics of particles, Cambridge, Cambridge, 1995.

[2] H. Morgan, N. G. Green, AC electrokinetic: colloids and nanoparticles, Research Studies Press, 2002.

[3] * K. D. Hermanson, S. O. Lumsdon, J. P. Williams, E. W. Kaler, O. D. Velev, Dielectrophoretic assembly of electrically functional microwires from nanoparticle suspensions, Science 294 (5544) (2001) 1082–1086.

[4] * B. C. Gierhart, D. G. Howitt, S. J. Chen, R. L. Smith, S. D. Collins, Frequency dependence of gold nanoparticle superassembly by dielectrophoresis, Langmuir 23 (24) (2007) 12450–12456.

[5] S. Gangwal, O. J. Cayre, O. D. Velev, Dielectrophoretic assembly of metallodielectric janus particles in ac electric fields, Langmuir 24 (23) (2008) 13312–13320.

[6] S. Gangwal, A. Pawar, I. Kretzschmar, O. D. Velev, Programmed assembly of metallodielectric patchy particles in external ac electric fields, Soft Matter 6 (7) (2010) 1413–1418.

[7] Y. Cui, Q. Wei, H. Park, C. M. Lieber, Nanowire nanosensors for highly sensitive and selective detection of biological and chemical species, Science 293 (5533) (2001) 1289–1292.

[8] Y. Li, F. Qian, J. Xiang, C. M. Lieber, Nanowire electronic and optoelectronic devices, Materials today 9 (10) (2006) 18–27.

[9] M. Law, L. E. Greene, J. C. Johnson, R. Saykally, P. Yang, Nanowire dye-sensitized solar cells, Nature materials 4 (6) (2005) 455–459.

[10] * P. A. Smith, C. D. Nordquist, T. N. Jackson, T. S. Mayer, B. R. Martin, J. Mbindyo, T. E. Mallouk, Electric-field assisted assembly and alignment of metallic nanowires, Applied Physics Letters 77 (9) (2000) 1399–1401.

[11] * D. Fan, F. Zhu, R. Cammarata, C. Chien, Controllable high-speed rotation of nanowires, Physical review letters 94 (24) (2005) 247208.

[12] B. Edwards, N. Engheta, S. Evoy, Electric tweezers: Experimental study of positive dielectrophoresis-based positioning and orientation of a nanorod, Journal of Applied Physics 102 (2) (2007) 024913.

[13] * R. Krupke, F. Hennrich, H. v. Löhneysen, M. M. Kappes, Separation of metallic from semiconducting single-walled carbon nanotubes, Science 301 (5631) (2003) 344–347.

[14] ** P. García-Sánchez, J. J. Arcenegui, H. Morgan, A. Ramos, Self-assembly of metal nanowires induced by alternating current electric fields, Applied Physics Letters 106 (2) (2015) 023110.

[15] T. Honegger, K. Berton, E. Picard, D. Peyrade, Determination of clausius–mossotti factors and surface capacitances for colloidal particles, Applied Physics Letters 98 (18) (2011) 181906.

[16] J. Boote, S. Evans, Dielectrophoretic manipulation and electrical characterization of gold nanowires, Nanotechnology 16 (9) (2005) 1500.

[17] * D. Fan, F. Zhu, R. Cammarata, C. Chien, Efficiency of assembling of nanowires in suspension by ac electric fields, Applied physics letters 89 (22) (2006) 223115.

[18] D. Fan, F. Q. Zhu, X. Xu, R. C. Cammarata, C. Chien, Electronic properties of nanoentities revealed by electrically driven rotation, Proceedings of the National Academy of Sciences 109 (24) (2012) 9309–9313.

[19] * Y. K. Ren, D. Morganti, H. Y. Jiang, A. Ramos, H. Morgan, Electrorotation of metallic microspheres, Langmuir 27 (6) (2011) 2128–2131.

[20] ** J. J. Arcenegui, P. García-Sánchez, H. Morgan, A. Ramos, Electroorientation and electrorotation of metal nanowires, Physical Review E 88 (6) (2013) 063018.

[21] A. J. Bard, L. R. Faulkner, Electrochemical methods: fundamentals and applications, Vol. 2, Wiley New York, 1980.

[22] ** A. Ramos, H. Morgan, N. G. Green, A. Castellanos, Ac electric-field-induced fluid flow in microelectrodes, Journal of colloid and interface science 217 (2) (1999) 420–422.

[23] ** M. Z. Bazant, K. Thornton, A. Ajdari, Diffuse-charge dynamics in electrochemical systems, Physical Review E 70 (2) (2004) 021506.

[24] J. Lyklema, Fundamentals of interface and colloid science. Volume II: Solid-liquid interfaces, Academic press, 1995.

[25] V. Shilov, V. Estrela-Lópis, Theory of movement of spherical particles of a suspension in an inhomogeneous electric field, Research in Surface Forces 4 (1975) 121.

[26] * V. Shilov, T. Simonova, Polarization of electric double-layer of disperse particles and dipolophoresis in a steady (dc) field, COLLOID JOURNAL OF THE USSR 43 (1) (1981) 90–96.

[27] H. A. Pohl, Dielectrophoresis: the behavior of neutral matter in nonuniform electric fields, Vol. 80, Cambridge university press Cambridge, 1978.

[28] * M. Z. Bazant, T. M. Squires, Induced-charge electrokinetic phenomena: theory and microfluidic applications, Physical Review Letters 92 (6) (2004) 066101.

[29] V. G. Levich, Physicochemical hydrodynamics, Prentice-Hall Englewood Cliffs, NJ, 1962.

[30] N. Gamayunov, V. Murtsovkin, A. Dukhin, Pair interaction of particles in electric field. 1. features of hydrodynamic interaction of polarized particles, Colloid J. USSR (Engl. Transl.);(United States) 48 (2).

[31] V. Murtsovkin, Nonlinear flows near polarized disperse particles, Colloid journal of the Russian Academy of Sciences 58 (3) (1996) 341–349.

[32] * N. Gamayunov, G. Mantrov, V. Murtsovkin, Study of flows induced in the vicinity of conducting particles by an extenal electric field, Colloid journal of the Russian Academy of Sciences 54 (1) (1992) 20–23.

[33] * A. Ajdari, Pumping liquids using asymmetric electrode arrays, Physical Review E 61 (1) (2000) R45.

[34] N. Green, A. Ramos, A. Gonzalez, H. Morgan, A. Castellanos, Fluid flow induced by nonuniform ac electric fields in electrolytes on microelectrodes. i. experimental measurements, Physical review E 61 (4) (2000) 4011.

[35] * A. Gonzalez, A. Ramos, N. Green, A. Castellanos, H. Morgan, Fluid flow induced by nonuniform ac electric fields in electrolytes on microelectrodes. ii. a linear double-layer analysis, Physical review E 61 (4) (2000) 4019.

[36] A. Brown, C. Smith, A. Rennie, Pumping of water with ac electric fields applied to asymmetric pairs of microelectrodes, Physical review E 63 (1) (2000) 016305.

[37] N. G. Green, A. Ramos, A. Gonzalez, H. Morgan, A. Castellanos, Fluid flow induced by nonuniform ac electric fields in electrolytes on microelectrodes. iii. observation of streamlines and numerical simulation, Physical review E 66 (2) (2002) 026305.

[38] A. Ramos, A. Gonzalez, A. Castellanos, N. G. Green, H. Morgan, Pumping of liquids with ac voltages applied to asymmetric pairs of microelectrodes, Physical Review E 67 (5) (2003) 056302.

[39] V. Studer, A. Pépin, Y. Chen, A. Ajdari, An integrated ac electrokinetic pump in a microfluidic loop for fast and tunable flow control, Analyst 129 (10) (2004) 944–949.

[40] T. M. Squires, M. Z. Bazant, Induced-charge electro-osmosis, Journal of Fluid Mechanics 509 (2004) 217–252.

[41] J. A. Levitan, S. Devasenathipathy, V. Studer, Y. Ben, T. Thorsen, T. M. Squires, M. Z. Bazant, Experimental observation of induced-charge electro-osmosis around a metal wire in a microchannel, Colloids and Surfaces A: Physicochemical and Engineering Aspects 267 (1) (2005) 122–132.

[42] ** T. M. Squires, M. Z. Bazant, Breaking symmetries in induced-charge electro-osmosis and electrophoresis, Journal of Fluid Mechanics 560 (2006) 65–101.

[43] ** D. Saintillan, E. Darve, E. S. Shaqfeh, Hydrodynamic interactions in the induced-charge electrophoresis of colloidal rod dispersions, Journal of Fluid Mechanics 563 (2006) 223–259.

[44] E. Yariv, Slender-body approximations for electro-phoresis and electro-rotation of polarizable particles, Journal of Fluid Mechanics 613 (2008) 85–94.

[45] ** S. Gangwal, O. J. Cayre, M. Z. Bazant, O. D. Velev, Induced-charge electrophoresis of metallodielectric particles, Physical review letters 100 (5) (2008) 058302.

[46] * T. Miloh, A unified theory of dipolophoresis for nanoparticles, Physics of Fluids (1994-present) 20 (10) (2008) 107105.

[47] E. Yariv, T. Miloh, Electro-convection about conducting particles, Journal of Fluid Mechanics 595 (2008) 163–172.

[48] ** T. Miloh, Nonlinear alternating electric field dipolophoresis of spherical nanoparticles, Physics of Fluids (1994-present) 21 (7) (2009) 072002.

[49] H. A. Stone, A. D. Stroock, A. Ajdari, Engineering flows in small devices: microfluidics toward a lab-on-a-chip, Annu. Rev. Fluid Mech. 36 (2004) 381–411.

[50] * M. Z. Bazant, T. M. Squires, Induced-charge electrokinetic phenomena, Current Opinion in Colloid & Interface Science 15 (3) (2010) 203–213.

[51] J. Gunning, D. Y. Chan, L. R. White, The impedance of the planar diffuse double layer: an exact low-frequency theory, Journal of colloid and interface science 170 (2) (1995) 522–537.

[52] A. Delgado, F. González-Caballero, R. Hunter, L. Koopal, J. Lyklema, Measurement and interpretation of electrokinetic phenomena (iupac technical report), Pure and Applied Chemistry 77 (10) (2005) 1753–1805.

[53] M. Z. Bazant, M. S. Kilic, B. D. Storey, A. Ajdari, Towards an understanding of induced-charge electrokinetics at large applied voltages in concentrated solutions, Advances in Colloid and Interface Science 152 (1) (2009) 48–88.

[54] A. J. Pascall, T. M. Squires, Induced charge electro-osmosis over controllably contaminated electrodes, Physical review letters 104 (8) (2010) 088301.

[55] Y. Suh, S. Kang, Numerical prediction of ac electro-osmotic flows around polarized electrodes, Physical Review E 79 (4) (2009) 046309.

[56] R. Messinger, T. Squires, Suppression of electro-osmotic flow by surface roughness, Physical review letters 105 (14) (2010) 144503.

[57] O. Schnitzer, E. Yariv, Induced-charge electro-osmosis beyond weak fields, Physical Review E 86 (6) (2012) 061506.

[58] L. H. Olesen, H. Bruus, A. Ajdari, ac electrokinetic micropumps: The effect of geometrical confinement, faradaic current injection, and nonlinear surface capacitance, Physical Review E 73 (5) (2006) 056313.

[59] A. Ramos, A. González, P. García-Sánchez, A. Castellanos, A linear analysis of the effect of faradaic currents on traveling-wave electroosmosis, Journal of colloid and interface science 309 (2) (2007) 323–331.

[60] S. M. Davidson, M. B. Andersen, A. Mani, Chaotic induced-charge electro-osmosis, Physical review letters 112 (12) (2014) 128302.

[61] J. Happel, H. Brenner, Low Reynolds number hydrodynamics, Martinus Nijhoff Publishers, 1983.

[62] M. Fair, J. Anderson, Electrophoresis of nonuniformly charged ellipsoidal particles, Journal of colloid and interface science 127 (2) (1989) 388–400.

[63] F. F. Reuss, Sur un nouvel effet de l'électricité galvanique, Mem. Soc. Imp. Natur. Moscou 2 (1809) 327–337.

[64] C. Peng, I. Lazo, S. V. Shiyanovskii, O. D. Lavrentovich, Induced-charge electro-osmosis around metal and janus spheres in water: Patterns of flow and breaking symmetries, Physical Review E 90 (5) (2014) 051002.

[65] ** P. García-Sánchez, Y. Ren, J. J. Arcenegui, H. Morgan, A. Ramos, Alternating current electrokinetic properties of gold-coated microspheres, Langmuir 28 (39) (2012) 13861–13870.

[66] A. Ramos, H. Morgan, N. G. Green, A. Castellanos, Ac electrokinetics: a review of forces in microelectrode structures, Journal of Physics D: Applied Physics 31 (18) (1998) 2338.

[67] L. Zheng, S. Li, J. P. Brody, P. J. Burke, Manipulating nanoparticles in solution with electrically contacted nanotubes using dielectrophoresis, Langmuir 20 (20) (2004) 8612–8619.

[68] D. Fan, F. Zhu, R. Cammarata, C. Chien, Manipulation of nanowires in suspension by ac electric fields, Applied Physics Letters 85 (18) (2004) 4175–4177.

[69] S. J. Papadakis, Z. Gu, D. H. Gracias, Dielectrophoretic assembly of reversible and irreversible metal nanowire networks and vertically aligned arrays, Applied Physics Letters 88 (23) (2006) 233118.

[70] * C. Akin, J. Yi, L. C. Feldman, C. Durand, S. M. Hus, A.-P. Li, M. A. Filler, J. W. Shan, Contactless determination of electrical conductivity of one-dimensional nanomaterials by solution-based electro-orientation spectroscopy, ACS nano 9 (5) (2015) 5405–5412.

[71] * T. Miloh, B. W. Goldstein, Electro-phoretic rotation and orientation of polarizable spheroidal particles in ac fields, Physics of Fluids (1994-present) 27 (2) (2015) 022003.

[72] * R. J. Castellano, C. Akin, G. Giraldo, S. Kim, F. Fornasiero, J. W. Shan, Electrokinetics of scalable, electric-field-assisted fabrication of vertically aligned carbon-nanotube/polymer composites, Journal of Applied Physics 117 (21) (2015) 214306.

[73] * K. A. Rose, J. A. Meier, G. M. Dougherty, J. G. Santiago, Rotational electrophoresis of striped metallic microrods, Physical Review E 75 (1) (2007) 011503.

[74] ** K. A. Rose, B. Hoffman, D. Saintillan, E. S. Shaqfeh, J. G. Santiago, Hydrodynamic interactions in metal rodlike-particle suspensions due to induced charge electroosmosis, Physical Review E 79 (1) (2009) 011402.

[75] * J. J. Arcenegui, P. García-Sánchez, H. Morgan, A. Ramos, Electro-orientation of a metal nanowire counterbalanced by thermal torques, Physical Review E 89 (6) (2014) 062306.

[76] N. G. Loucaides, A. Ramos, Wall effects on the electrical manipulation of metal nanowires, Electrophoresis 36 (13) (2015) 1414–1422.

[77] A. Boymelgreen, G. Yossifon, S. Park, T. Miloh, Spinning janus doublets driven in uniform ac electric fields, Physical Review E 89 (1) (2014) 011003.

[78] P. García-Sánchez, A. Ramos, Electrorotation of a metal sphere immersed in an electrolyte of finite debye length, Physical Review E 92 (5) (2015) 052313.

[79] * J. J. Arcenegui, A. Ramos, P. García-Sánchez, H. Morgan, Electrorotation of titanium microspheres, Electrophoresis 34 (7) (2013) 979–986.

[80] * J. J. Arcenegui, P. García-Sánchez, H. Morgan, A. Ramos, Electric-field-induced rotation of brownian metal nanowires, Physical Review E 88 (3) (2013) 033025.

[81] R. Kretschmer, W. Fritzsche, Manipulation of metal nanoparticles in micrometer electrode gaps by dielectrophoresis, in: DNA-BASED MOLECULAR ELECTRONICS: International Symposium on DNA-Based Molecular Electronics, Vol. 725, AIP Publishing, 2004, pp. 85–87.

[82] R. Kretschmer, W. Fritzsche, Pearl chain formation of nanoparticles in microelectrode gaps by dielectrophoresis, Langmuir 20 (26) (2004) 11797–11801.

[83] N. Ranjan, H. Vinzelberg, M. Mertig, Growing one-dimensional metallic nanowires by dielectrophoresis, Small 2 (12) (2006) 1490–1496.

[84] N. Khanduja, S. Selvarasah, C.-L. Chen, M. R. Dokmeci, X. Xiong, P. Makaram, A. Busnaina, Three dimensional controlled assembly of gold

nanoparticles using a micromachined platform, Applied physics letters 90 (8) (2007) 83105–83105.

[85] L. Bernard, M. Calame, S. van der Molen, J. Liao, C. Schönenberger, Controlled formation of metallic nanowires via au nanoparticle ac trapping, Nanotechnology 18 (23) (2007) 235202.

[86] R. J. Barsotti, M. D. Vahey, R. Wartena, Y.-M. Chiang, J. Voldman, F. Stellacci, Assembly of metal nanoparticles into nanogaps, small 3 (3) (2007) 488–499.

[87] J. Puigmartí-Luis, J. Stadler, D. Schaffhauser, Á. P. Del Pino, B. R. Burg, P. S. Dittrich, Guided assembly of metal and hybrid conductive probes using floating potential dielectrophoresis, Nanoscale 3 (3) (2011) 937–940.

[88] H. Ding, W. Liu, J. Shao, Y. Ding, L. Zhang, J. Niu, Influence of induced-charge electrokinetic phenomena on the dielectrophoretic assembly of gold nanoparticles in a conductive-island-based microelectrode system, Langmuir 29 (39) (2013) 12093–12103.

[89] E. M. Freer, O. Grachev, X. Duan, S. Martin, D. P. Stumbo, High-yield self-limiting single-nanowire assembly with dielectrophoresis, Nature Nanotechnology 5 (7) (2010) 525–530.

[90] P. Stokes, S. I. Khondaker, Directed assembly of solution processed single-walled carbon nanotubes via dielectrophoresis: from aligned array to individual nanotube devices, Journal of Vacuum Science & Technology B 28 (6) (2010) C6B7–C6B12.

[91] M. Li, R. B. Bhiladvala, T. J. Morrow, J. A. Sioss, K.-K. Lew, J. M. Redwing, C. D. Keating, T. S. Mayer, Bottom-up assembly of large-area nanowire resonator arrays, Nature Nanotechnology 3 (2) (2008) 88–92.

[92] B. D. Smith, T. S. Mayer, C. D. Keating, Deterministic assembly of functional nanostructures using nonuniform electric fields, Annual review of physical chemistry 63 (2012) 241–263.

[93] L. Zhang, Y. Zhu, Directed assembly of janus particles under high frequency ac-electric fields: Effects of medium conductivity and colloidal surface chemistry, Langmuir 28 (37) (2012) 13201–13207.

Figure 1

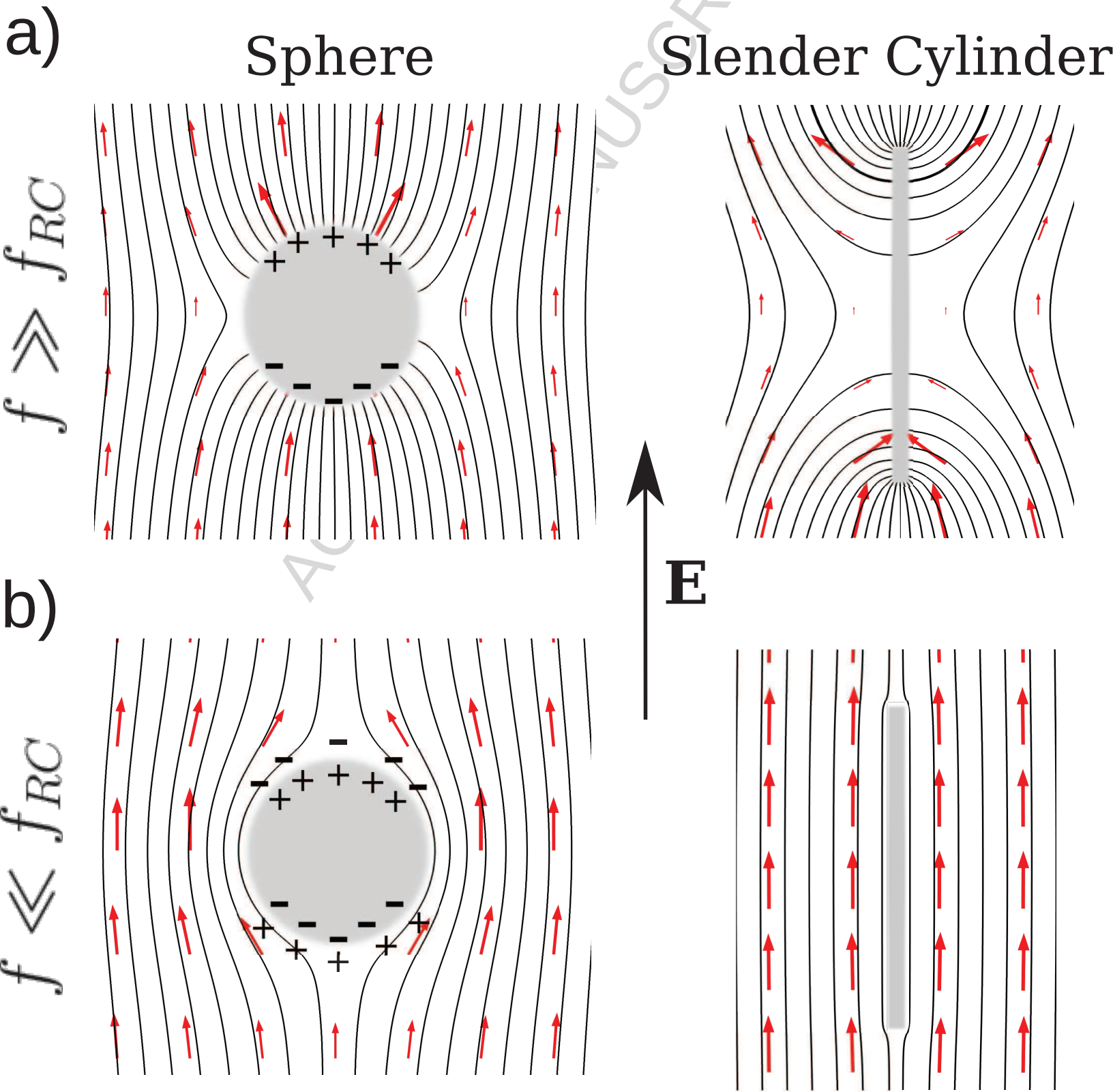

Figure 1: a) Left and right figures show the electric field lines for high frequencies of the AC signal ($f \gg f_{RC}$) for a conducting sphere and for a conducting cylinder, respectively. In this case the perturbation of the electric field is important for both the sphere and the cylinder. b) Left and right figures show the electric field lines at low frequencies ($f \ll f_{RC} \equiv 2\pi/t_{RC}$). Electric field lines surround the particles. In the case of a slender cylinder the electric field is only very slightly perturbed and, consequently, the induced dipole is small.

Figure 2

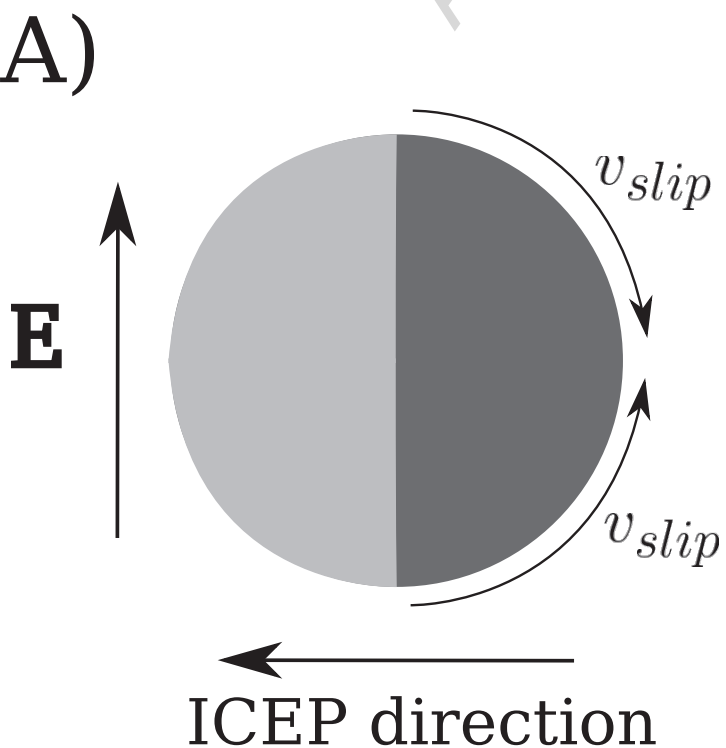

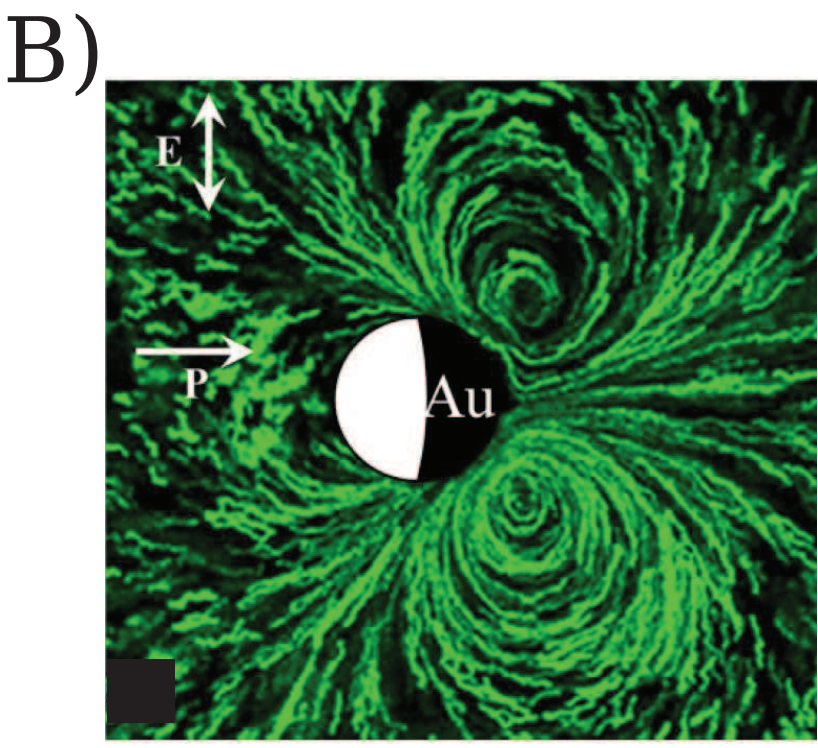

Figure 2: a) Schematic representation of a metallodillectic (Janus) particle subjected to an AC field. The metal-dielectric interface aligns with the field direction and ICEO flows appear on the metal side. As a consequence of these flows, the Janus particle moves towards the dielectric side (ICEP motion). b) Experimental ICEO streamlines for a Janus sphere with 50 micron diameter subjected to an electric field of 5 kV/m (reproduced from [64], Copyright 2014 American Physical Society).

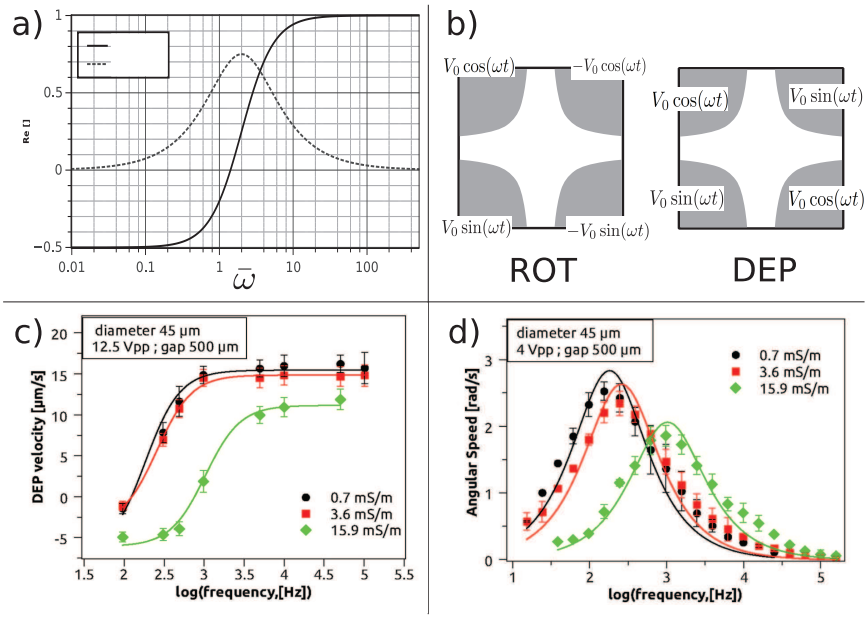

Figure 3: a) Nondimensional polarizability $\bar{\alpha}$ as a function of nondimensional frequency $\bar{\omega}$; b) Schematic diagram of four-electrode array and applied voltages for ROT and DEP experiments; c) DEP velocity as a function of frequency; d) ROT angular velocity as a function of frequency, (Figs. c, d reproduced from [65], Copyright 2012 American Chemical Society)

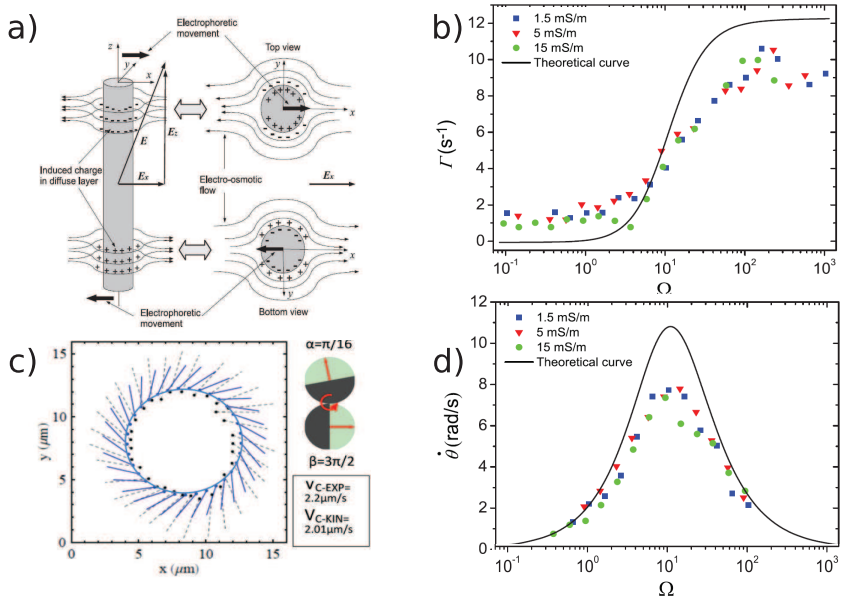

Figure 4: a)ICEO flows around a metal nanowire induce the orientation of the nanowire. The upper part can be described as a metal particle undergoing electrophoresis to the right, while the lower part moves to the left. b) Electro-orientation rates as a function of nondimensional frequency for Ag nanowires. Applied field was about 10 kV/m. c)Rotation and translation of a Janus doublet subjected to a unidirectional field. The applied field (13.4 kV/m and 1.5 kHz) is perpendicular to the plane of view. d) Electro-rotation rates as a function of nondimensional frequency for Ag nanowires. Applied field about 10 kV/m. (Figs. a, b, d reproduced from [20], Copyright 2013 American Physical Society; fig. c reproduced from [77], Copyright 2014 American Physical Society)

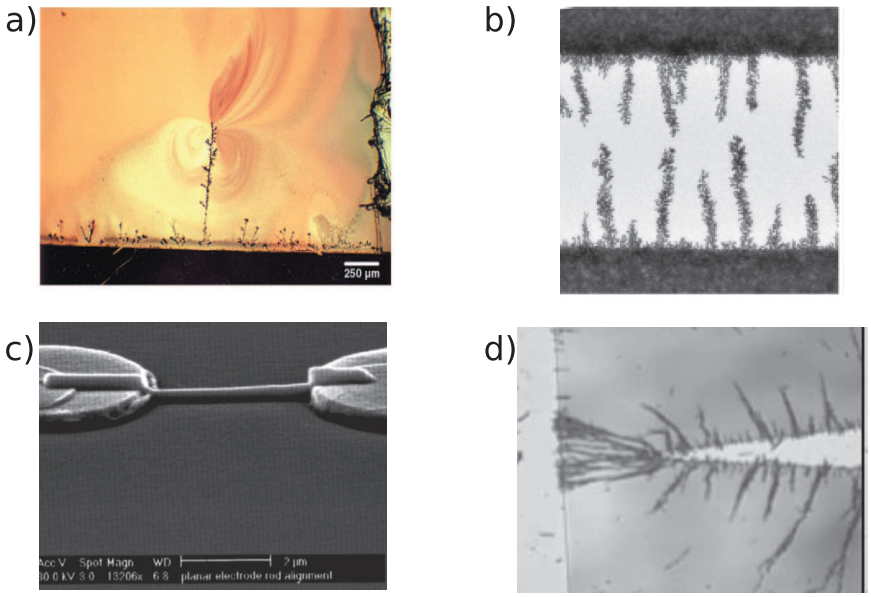

Figure 5: a) Dielectrophoretic assembly of metal colloids to form a microwire. The formation is very quick and it can be used to bridge the gap between microelectrodes (applied field $\approx$ 250 V/cm). (Reproduced from [3], Copyright 2001 AAAS). b) Assembly of 15.5 nm gold nanoparticles on microelectrodes with 3 μm gap. AC electroosmosis leads to assembly patterns that strongly depend on the signal frequency. The figure shows that long chains can be obtained for an AC signal with 7.5 V and 10 kHz. Reproduced from [4], Copyright 2007 Americal Chemical Society). c) Electrical manipulation of a single gold nanowire can be used to perform nanocontacts by bringing and placing the nanowire between microelectrodes.(Reproduced from [10], Copyright 2000 AIP Publishing). d) Assembly of Ag nanowires achieves electrical contact between microelectrodes with large gap (applied signal of 0.2 V and 100 kHz). (Reproduced from [69], Copyright 2006 AIP Publishing).

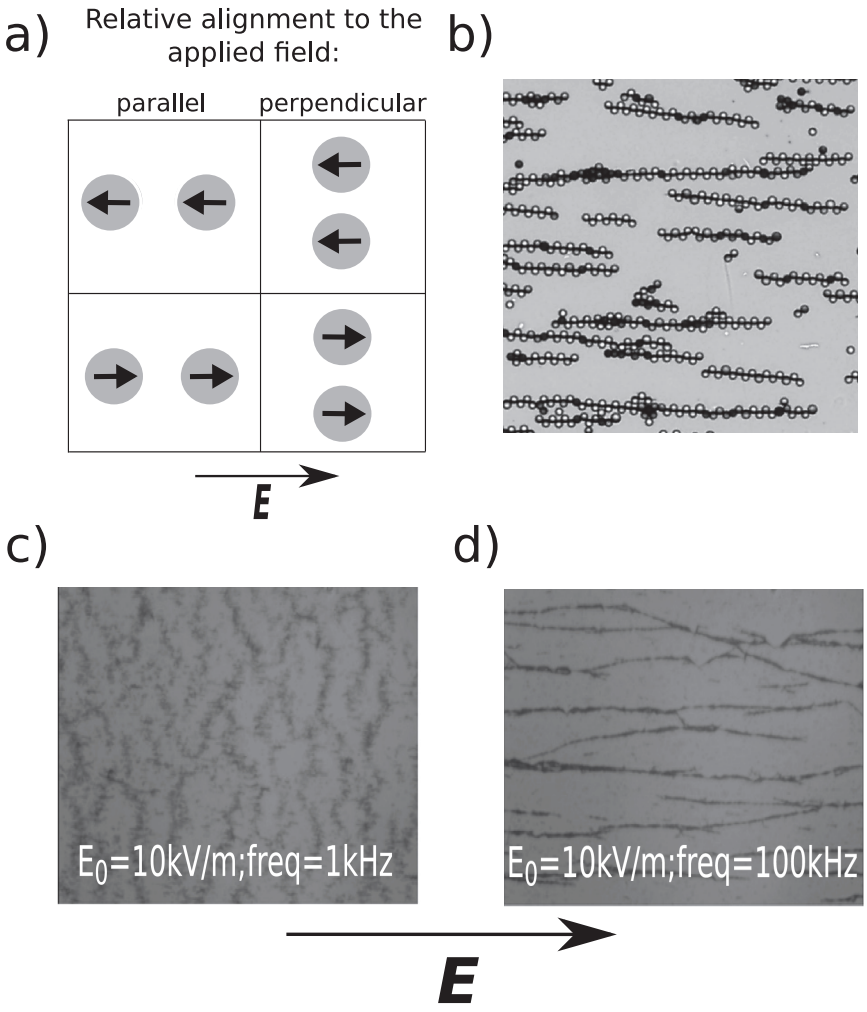

Figure 6: a) Either at low or high frequencies, dipole-dipole interactions lead to chaining of metal spheres. b) Pearl-chaining of Janus particles (Reproduced from [5], Copyright 2008 American Chemical Society). c) For low frequencies, silver nanowires form bands perpendicular to the direction of the applied field. d) At high frequencies, silver nanowires assemble into chains (Reproduced from [14], Copyright 2015 AIP Publishing)

Graphical abstract

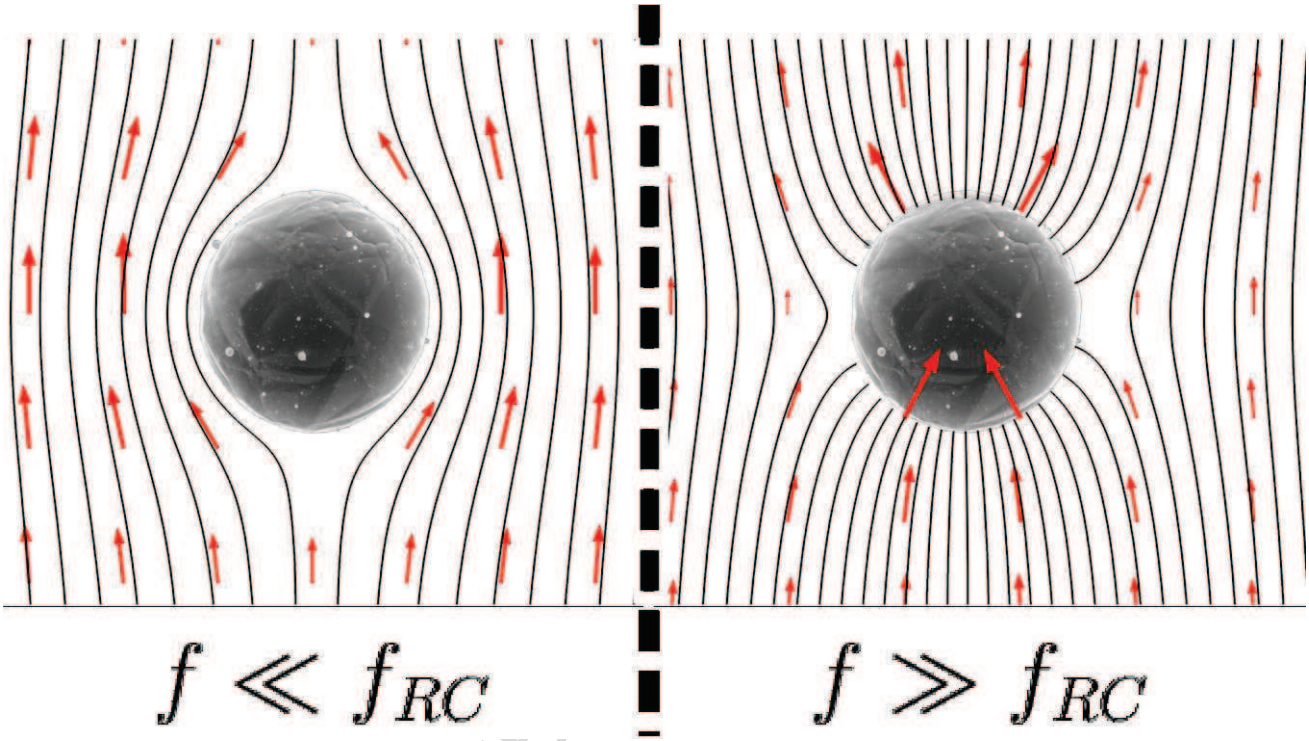

Highlights

- Experimental behavior and theory of metal microparticles are compared.
- Particle motion is due to electrical forces on induced charges in the double layer.
- Characteristic time is the RC time for charging the metal/electrolyte double layer.
- Electric-field driven assembly of conducting particles is reviewed.